Metabolism, Pharmacokinetics, Tissue Distribution, and Stability Studies of the Prodrug Analog of an Anti-Hepatitis B Virus Dinucleoside Phosphorothioate[S]

John E. Coughlin, Rajendra K. Pandey, Seetharamaiyer Padmanabhan,
Kathleen G. O'Loughlin, Judith Marquis, Carol E. Green, Jon C. Mirsalis, and
Radhakrishnan P. Iyer

*Spring Bank Pharmaceuticals, Inc., Milford, Massachusetts (J.E.C., R.K.P., S.P., R.P.I.); SRI International, Toxicology &
Pharmacokinetics, Menlo Park, California (K.G.O., C.E.G., J.C.M.); and Genzyme Corporation, Marlborough, Massachusetts (J.M.)*

ABSTRACT:

The alkoxycarbonyloxy dinucleotide prodrug R_p, S_p-2 is an orally bioavailable anti-hepatitis B virus agent. The compound is efficiently metabolized to the active dinucleoside phosphorothioate R_p, S_p-1 by human liver microsomes and S9 fraction without cytochrome P450-mediated oxidation or conjugation. The conversion of R_p, S_p-2 to R_p, S_p-1 appears to be mediated by liver esterases, occurs in a stereospecific manner, and is consistent with our earlier reported studies of serum-mediated hydrolytic conversion of R_p, S_p-2 to R_p, S_p-1. However, further metabolism of R_p, S_p-1 does not occur. The presence of a minor metabolite, the desulfurized product 10 was noted. The prodrug R_p, S_p-2 was quite stable in simulated gastric fluid, whereas the active R_p, S_p-1 had a half-life of <15 min. In simulated intestinal fluid, the prodrug 2 was fully converted to 1 in approximately 3 h, whereas 1 remained stable. To ascertain the tissue distribution of the prodrug 2 in rats, the synthesis of ^{35}S-labeled R_p, S_p-2 was undertaken. Tissue distribution studies of orally and intravenously administered radiolabeled [^{35}S]2 demonstrated that the radioactivity concentrates in the liver, with the highest liver/plasma ratio in the intravenous group at 1 h being 3.89 (females) and in the oral group at 1 h being 2.86 (males). The preferential distribution of the dinucleotide 1 and its prodrug 2 into liver may be attributed to the presence of nucleoside phosphorothioate backbone because phosphorothioate oligonucleotides also reveal a similar tissue distribution profile upon intravenous administration.

Introduction

Nucleotides are among the most important ligands for a number of intracellular and extracellular proteins involved in biochemical reactions and cell signaling (Saito et al., 2006). In addition, nucleic acid-protein interactions constitute essential events in a variety of cellular processes (Sanger, 1983; Ollis and White, 1987). Therefore, rationally designed agonists and antagonists of specific nucleotide-protein and nucleic acid-protein interactions should have broad therapeutic applications against multiple diseases (Ellington and Conrad, 1995).

Small molecule nucleic acid hybrids (SMNH), which are two to six nucleotides long, represent a new class of small molecule chemical entities that can be rationally designed to target key nucleotide-protein and nucleic acid-protein interactions involved in a disease process. Indeed, reports suggest that mono-, di-, tri-, and short-chain oligonucleotides (ODNs) possess significant and diverse biological activities that can be exploited for therapeutic applications (Wagner et al., 1996; Hannoush et al., 2004; Iyer et al., 2004, 2005b).

In previous studies, we have shown that in general, the SMNH class of molecules has unique metabolic and pharmacokinetic properties that are distinct from traditional small molecule drugs (Iyer et al., 2004a, 2006). Thus, in contrast to the hydrophobic small molecule compounds, which are subject to cytochrome P450 (P450)-mediated Phase I oxidative processes and Phase II conjugation reactions, SMNH analogs are not metabolized by P450 enzyme systems. Fur-

ABBREVIATIONS: SMNH, small molecule nucleic acid hybrids; P450, cytochrome P450; ODN, oligonucleotide; PS-ODN, phosphorothioate oligonucleotide; ADME, absorption, distribution, metabolism, and excretion; siRNA, small interfering RNA; HBV, hepatitis B virus; SGF, simulated gastric fluid; SIF, simulated intestinal fluid; DMT-N^{Bz}-dA, 5′-O-4,4-dimethoxytriphenylmethyl-N^6-benzoyl-2′-deoxyadenosine; ETT, 5-ethylthiotetrazole; DCA, dichloroacetic acid; DCM, dichloromethane; CPG, controlled pore glass; DMT-T, 5′-O-4,4-dimethoxytriphenylmethyl-thymidine; dA, 2′-deoxyadenosine; HPLC, high-performance liquid chromatography; MS, mass spectrometry; LC/MS, liquid chromatography/mass spectrometry; AUC, area under the plasma concentration-time profile; C_{max}, maximal plasma concentration.

thermore, in in vivo studies, we have reported that a representative dinucleoside phosphorothioate **1** does not seem to be metabolized by Phase I or Phase II processes and is mostly eliminated as intact compound (Iyer et al., 2006). Lack of P450 metabolism of SMNH molecules is a unique pharmaceutical attribute that confers distinct advantages in that such molecules are not subject to the "first-pass effect," and they can be combined with different classes of drugs without the potential for drug-drug interactions (Gibaldi et al., 1971). In the context of antiviral therapeutics, a cocktail of drugs each with unique mechanisms of action that can act synergistically with minimal toxicity is particularly important for the treatment of chronic infections (Perrillo, 2004). Consequently, the development of SMNH analogs as antiviral agents is of great interest.

SMNH compounds are small molecule counterparts of the more widely studied class of long-chain phosphorothioate oligonucleotides (PS-ODN). Extensive absorption, distribution, metabolism, and excretion (ADME) studies of PS-ODN reveal a pattern in which after intravenous administration, they are 1) rapidly cleared from plasma after absorption, 2) preferentially distributed to liver, kidney, spleen, and bone marrow, 3) metabolized by *exo-* and *endo-*nucleases into shorter ODN fragments, and 4) excreted primarily through kidneys (Crooke et al., 2000; Peng et al., 2001; Geary, 2009). Studies of duplexed synthetic ODNs as small interfering RNA (siRNA) (Tuschl, 2001; Hannon, 2002) show a similar ADME trend, although the overall pharmacokinetic and tissue distribution profile is dependent on the extent of chemical modification and the conjugating moieties (van de Water et al., 2006; Li and Liang, 2010). It was therefore of interest to evaluate the ADME properties of SMNH compounds.

Chemically modified antisense ODNs (Szymkowski, 1996; Dias and Stein, 2002) as "hybrid" or "gapmers" have been reported to be orally bioavailable in vivo (Agrawal et al., 1995; Tillman et al., 2008), although the extent of pharmaceutical bioavailability and mechanisms of absorption are not known. In contrast, in vitro studies using Caco-2 cell lines and in vivo studies in rats revealed that none of the SMNH analogs has potential for oral bioavailability, presumably because of the negative charge(s) on their backbone that impedes their passive diffusion across the cellular lipid bilayer (Iyer et al., 2004a, 2006; Coughlin et al., 2010).

As part of further development of the SMNH compounds, we have undertaken preclinical studies to develop the anti-hepatitis B virus (HBV) SMNH analog **1** as an orally bioavailable compound. The analog **1** was not stable in simulated gastric fluid (SGF), because of its susceptibility to acid-catalyzed depurination, but was stable in simulated intestinal fluid (SIF). An ideal SMNH analog is required to be stable in the gastrointestinal tract; therefore, the development of a prodrug strategy for oral delivery appeared logical.

We have reported the synthesis and evaluation of various orally bioavailable prodrug derivatives of **1** (Padmanabhan et al., 2006). These analogs are designed to mask the negative charge on the backbone of the dinucleotide and to improve their hydrophobicity to facilitate passive diffusion through cell membrane. As a part of the continuing development of a prodrug analog **2**, we evaluated its ADME properties, its stability in SGF and SIF, and its oral bioavailability. The results are presented here.

Materials and Methods

Materials for Chemical Synthesis. 5′-*O*-4,4′-Dimethoxytriphenylmethyl-*N*^{6}-benzoyl-2′-deoxyadenosine (DMT-*N*^{Bz}-dA), 5′-*O*-4,4′-dimethoxytriphenylmethyl-thymidine (DMT-T), and 4,4′-dimethoxytriphenylmethyl-2′-*O*-methyl-uridine (DMT-U$_{2′-OMe}$) were obtained from Reliable Biopharmaceuticals (St. Louis, MO) and were used as such. T-phosphoramidite monomer was obtained from Rasayan Chemicals (Encinitas, CA). Anhydrous pyridine, triethylamine, and

dimethylformamide, obtained from Sigma-Aldrich (St. Louis, MO) were freshly distilled from CaH$_2$ before use. Other reagents such as 1-ethyl-3-(3-dimethylaminopropyl) carbodiimide, *N,N*-dimethylaminopyridine, 5-ethylthio-tetrazole (ETT), dichloroacetic acid (DCA), and triethylamine were obtained from Sigma-Aldrich and were used as received. Controlled pore glass (CPG) support was obtained from Prime Synthesis, Inc. (Aston, PA). Capping reagent A and capping reagent B were obtained from American International Chemicals (Natick, MA).

Synthesis of the Dinucleotide 1. The dinucleotide **1** was synthesized on a multimillimole scale using 2′-deoxyadenosine (dA)-loaded CPG support in conjunction with solid-phase phosphoramidite chemistry (Beaucage and Iyer, 1992) (Fig. 1). For the synthesis, we used a specially fabricated LOTUS reactor as described previously (Iyer et al., 2005a). Nucleoside-loaded support (112 g, 89 mmol) prepared as described previously (Padmanabhan et al., 2005) was detritylated using DCA in dichloromethane (DCM) (2.5%, DCA/DCM, 3 × 400 ml) with DCM washes (3 × 400 ml) between each DCA/DCM treatment, and the support was subsequently washed thoroughly with DCM (5 × 400 ml) and later with acetonitrile (low water, <30 ppm). Detritylated nucleoside was coupled with 2′-*O*-methyluridine phosphoramidite (5 Eq) in the presence of ETT (0.4 M, 10 Eq) in anhydrous acetonitrile under argon. After acetonitrile washings, sulfurization was performed using 3*H*-benzodithiole-3-one-1,1-dioxide reagent (5 Eq) (Iyer et al., 1990a,b) to give the fully protected CPG-bound dinucleotide. The 5′-DMT group was removed using 2.5% DCA/DCM (3 × 400 ml), and the CPG was washed with DCM (5 × 400 ml), acetonitrile (3 × 400 ml), and finally water (3 × 500 ml). The dinucleotide **1** was released from the support by deprotection and cleavage using NH$_4$OH (200 ml, 28–30%) at ~30°C under orbital shaking overnight. The ammoniacal solution was acidified with glacial acetic acid to pH 6 under cooling followed by filtration to give crude **1**, which was purified by three-stage preparative high-performance liquid chromatography (HPLC) as described below.

Desalting of the dinucleotide **1** solution was performed in a 500-ml stainless steel C-18 column. Initially, the column was equilibrated with NH$_4$OAc (0.1 M, pH 7.0, at a flow rate of 20 ml/min) followed by loading of dinucleotide **1** solution. The dinucleotide **1** was eluted from the column using a gradient of acetonitrile and water. The desalted dinucleotide **1** solution was concentrated to 20% of volume in vacuo, diluted with water, and was subjected to ion-exchange chromatography using Toyopearl Super Q 650M resin (Tosoh Bioscience, King of Prussia, PA). After equilibration of the column with NaOAc (0.1 M), **1** was loaded onto the column, which was washed with 3 column volumes of NaOAc (0.1 M, pH 7.0). The dinucleotide **1** was eluted with NaOAc (0.1 M) and NaCl (1 M) buffer and was further purified by reversed-phase HPLC on a C-18 column. The sodium salt of **1** was eluted with acetonitrile/water (20:80). The eluent was lyophilized to obtain the dinucleotide **1** as a white fluffy solid.

Synthesis of 2. The prodrug **2** was prepared by the *S*-alkylation of the dinucleotide **1** with iodomethyl isopropyl carbonate (**3**). The iodo-compound **3** was prepared as described previously (Padmanabhan et al., 2006). The product **3** was characterized by ^{1}H nuclear magnetic resonance (NMR), ^{13}C NMR, and mass spectrometry (MS). ^{1}H NMR (CDCl$_3$): δ 1.2 ppm (6H, s), 4.8 (1H, m), 5.8 (2 H, s); ^{13}C NMR (CDCl$_3$): δ 154, 76, 36, and 22 ppm; electrospray ionization (positive mode)-MS, 244.

The *S*-alkylation protocol was essentially as described previously (Coughlin et al., 2010). After HPLC purification, **2** was obtained as a lyophilized powder as an R_p, S_p diastereomeric mixture (~55:45, 52%).

Spectral Data of R_p, S_p-2. ^{1}H NMR (CD$_3$OD), δ 1.16 (s, 3H), 1.24 (s, 3H), 2.49 (m, 1H), 2.89 (m, 1H), 3.45 (s, 3H), 3.75 (s, 2H), 4.21 (m, 1H), 4.3 (d, 1H), 4.45 (m, 2H), 4.77 (m, 1H), 4.85 (m, 1H), 5.15 (m, 1H), 5.42 (d, 1H), 5.44 (d, 1H), 5.71 (d, 1H), 6.01 (d, 1H), 6.46 (t, 1H), 7.98 (d, 1H), 8.21 (s, 1H), 8.29 (d, 1H) ppm; ^{13}C NMR (CD$_3$OD), δ 22.62, 40.68, 59.34, 59.42, 61.59, 61.84, 67.81, 67.92, 69.03, 72.35, 74.79, 76.78, 83.09, 83.14, 83.44, 85.22, 85.99, 86.11, 86.61, 103.39, 103.47, 120.52, 120.72, 141.09, 141.22, 142.28, 150.61, 152.39, 152.47, 154.00, 154.68, 154.93, 157.39, 165.06 ppm; ^{31}P NMR (CD$_3$OD), δ 27.7 and 28.6 ppm; MS, *m/z* 703.6.

Synthesis of Radiolabeled Compounds. *Synthesis of [^{35}S]2.* The dinucleoside phosphorothioate ester [^{35}S]**2** [34.2 mg, total activity 4.44 mCi (91.81 μCi/μmol)] was prepared by radiosynthesis (Fig. 1). The ^{35}S label was installed on the phosphorothioate backbone using ^{35}S-3*H*-benzodithiole-3-one-1,1-dioxide (Iyer et al., 1994). [^{35}S]**2** had a radiochemical purity of >98% as

FIG. 1. A, synthetic scheme depicting the solid-phase synthesis of 1. B, synthesis of the prodrug 2 from 1.

assessed by radio-HPLC (see Supplemental Fig. 1). Detailed methods of radiosynthesis and analysis are reported elsewhere (S.-W. Rhee, R. P. Iyer, J. E. Coughlin, S. Padmanabhan, J. P. Malerich, and M. J. Tanga, unpublished observations). All materials were stored at −20°C until ready to use.

In Vitro Metabolism and Stability Studies of 2. Metabolism studies using liver microsomes and S9 fractions were performed as described previously (Dalvie et al., 2009).

Materials. Pooled human liver microsomes, S9 from liver, NADPH, alamethicin, UDP-GlcUA, adenosine 3′-phosphate 5′-phosphosulfate lithium salt hydrate, S-(5′-adenosyl)-L-methionine iodide, CoASAc sodium salt, pepsin and pancreatin were purchased from Sigma-Aldrich.

The metabolite samples were analyzed by reversed-phase HPLC using Waters instrument equipped with 600E Controller, PDA 996 detector, Waters 717 Auto sampler with Millennium software (Waters, Milford, MA). A Waters Nova-Pak C18 4-μm (3.9 × 300 mm) column operating on a gradient of 100%

A (0.1 M ammonium acetate) to 100% B [0.1 M ammonium acetate/acetonitrile (20:80)] with a flow rate of 0.5 ml/min over 41 min was used.

Liquid Chromatography/mass spectrometry (LC/MS) analysis of the samples was performed on an Agilent 1100 Series HPLC with UV detection and MSD system (Agilent Technologies, Santa Clara, CA). For the liquid chromatography analysis of the samples, a Phenomenex Luna C18 column (5 μM, 4.6 × 250 mm) operating at 25°C was used (Phenomenex, Torrance, CA). Other chromatographic conditions were as follows: injection volume, 50 μl; elution gradient, 5 to 50% acetonitrile in 0.1 M NH$_4$OAc over 45 min; and flow rate, 0.5 ml/min. In the mass spectrum, the molecular mass signals represented [M + H] and/or [M + Na] ions. The MS instrument was an electrospray ionization, ion-trap mass spectrometer. The mass spectra were obtained in full ion-scan mode with a range between 100 and 1200 m/z. Other parameters were as follows: resolution, 13,000 m/z per s; dry temperature, 350°C; capillary ramp range, 1500 to 4500 V; nebulizer pressure, 60 psi; dry gas flow, 10 l/min;

trap target 30,000; and maximal accumulation time, 100 ms. Instrument calibration was verified using seven compounds of known molecular mass between 118 and 2722 Da. The predicted chemical formulae and calculated accurate mass were obtained from ChemDraw Standard 8.0 (CambridgeSoft Corporation, Cambridge, MA) on the basis of the proposed metabolic pathways and putative structures.

In Vitro Metabolism of 2 Using Liver Microsomes. A stock solution of prodrug **2** was prepared in deionized water at 1 mM concentration and diluted further to make a 10-μM solution. The incubation mixture contained liver microsomes (1 mg/ml), NADPH (1.3 mM), UDP-GlcUA (5 mM), alamethicin (10 μg/ml) in 1 ml of 1× phosphate-buffered saline buffer, at 10 μM final concentration of **2**. The liver microsomes were treated with alamethicin in an ice bath for 15 min before use. NADPH and UDP-GlcUA were added, and the incubate was maintained at 37°C in a shaking water bath. Samples were taken out at 1, 4, 6, and 8 h and were quenched with acetonitrile (2 ml). The resulting precipitate was removed by centrifugation for 10 min, and supernatant was lyophilized and reconstituted in 200 μl of water for HPLC analysis. The metabolite samples were also independently evaluated by LC/MS analysis.

Metabolism of 2 in S9 Fractions from Human Liver. The prodrug **2** (10 μM) was incubated with a mix containing S9 fraction (pooled from human) (1 mg/ml), NADPH (1.3 mM), UDP-GlcUA (5 mM), and alamethicin (10 μg/ml) in 1 ml of 1× PBS buffer. *S*-(5'-adenosyl)-L-methionine iodide (0.1 mM), adenosine 3'-phosphate 5'-phosphosulfate lithium salt hydrate (0.1 mM), and CoASAc (1 mM).

The S9 fraction was treated with alamethicin on ice for 15 min before use. Incubations were performed at 37°C in a shaking water bath. Samples were removed at 1, 4, and 6 h and were quenched with 2 ml of acetonitrile. After 60 min at room temperature, the resulting precipitate was removed by centrifugation. The supernatant was lyophilized and reconstituted in 200 μl of water for HPLC analysis. The lyophilized samples were also independently evaluated by LC/MS analysis.

Stability Studies of 2 in SGF and SIF. SGF and SIF were prepared as per The United States Pharmacopeia (1993). In brief, SGF was prepared by dissolving NaCl (2.0 g), purified pepsin (3.2 g, from porcine stomach mucosa), and HCl (36%, 7 ml) and diluting with water to 1 liter. This test solution had a pH of 1.2. For the preparation of SIF, monobasic potassium phosphate (6.8

g) was dissolved in water (250 ml), and NaOH (0.2 N, 77 ml) and H_2O (500 ml) were added. Pancreatin (10 g) was added and mixed, and the solution was adjusted to pH 6.8 with 0.2 N HCl and finally diluted with water to 1 liter.

A stock solution of **2** was prepared (2 mg in 100 μl of dimethyl sulfoxide). To 10 μl of stock solution, 200 μl of either SGF or SIF was added and incubated at 37°C. At different time points (15 min, 30 min, 1 h, and 3 h), aliquots were drawn and quenched with acetonitrile. The pH of the SGF sample was adjusted to 7.0 using ammonium acetate buffer. The precipitate was removed by centrifugation. The supernatant was lyophilized, and the residue was reconstituted in 200 μl of water for HPLC analysis as described before.

Tissue Distribution and Metabolism of [³⁵S]2. Tissue distribution and metabolism studies were performed using Sprague-Dawley rats obtained from Harlan (Livermore, CA) and Charles River Laboratories (Wilmington, MA). A total of 18 animals (9 males and 9 females), 8 to 13 weeks old, weighing 245 to 303 g were used. Animals were housed in a facility accredited by the Association for Assessment and Accreditation of Laboratory Animal Care. General procedures for animal care and housing were performed in accordance with the National Research Council *Guide for the Care and Use of Laboratory Animals* (Institute of Laboratory Animal Resources, 1996) and the Animal Welfare Standards incorporated in 9 Code of Federal Regulations Part 3, 1991. Animals destined for the 24-h sacrifice were housed in glass metabolism cages to allow for urine and feces collection. The light cycle was 12-h light/dark; the temperature range was 65–72°F; and the number of ventilations was 10 room volumes per hour, with no recirculation of air. Purina Certified Rodent Chow #5002 ad libitum was used (Purina, St. Louis, MO). Water (purified, reverse osmosis) was provided ad libitum.

The prodrug [³⁵S]**2** was administered by bolus intravenously via a tail vein or oral gavage at a single dose. The dosing volume was 5 ml/kg, and the experimental duration was 24 h. Evaluation parameters included radioactivity levels in blood, tissues, carcass, and excreta. For intravenous administration, the vehicle used was a mixture of 25% polyethylene glycol 400 and 75% sterile saline for injection (0.9% sodium chloride for injection; The United States Pharmacopeia, 1993), and that for oral administration was 0.05 M citric acid buffer, pH 2.5.

Formulations. Intravenous and oral dose formulation(s) were prepared by adding the appropriate amount of **2** in the vehicle to achieve the target
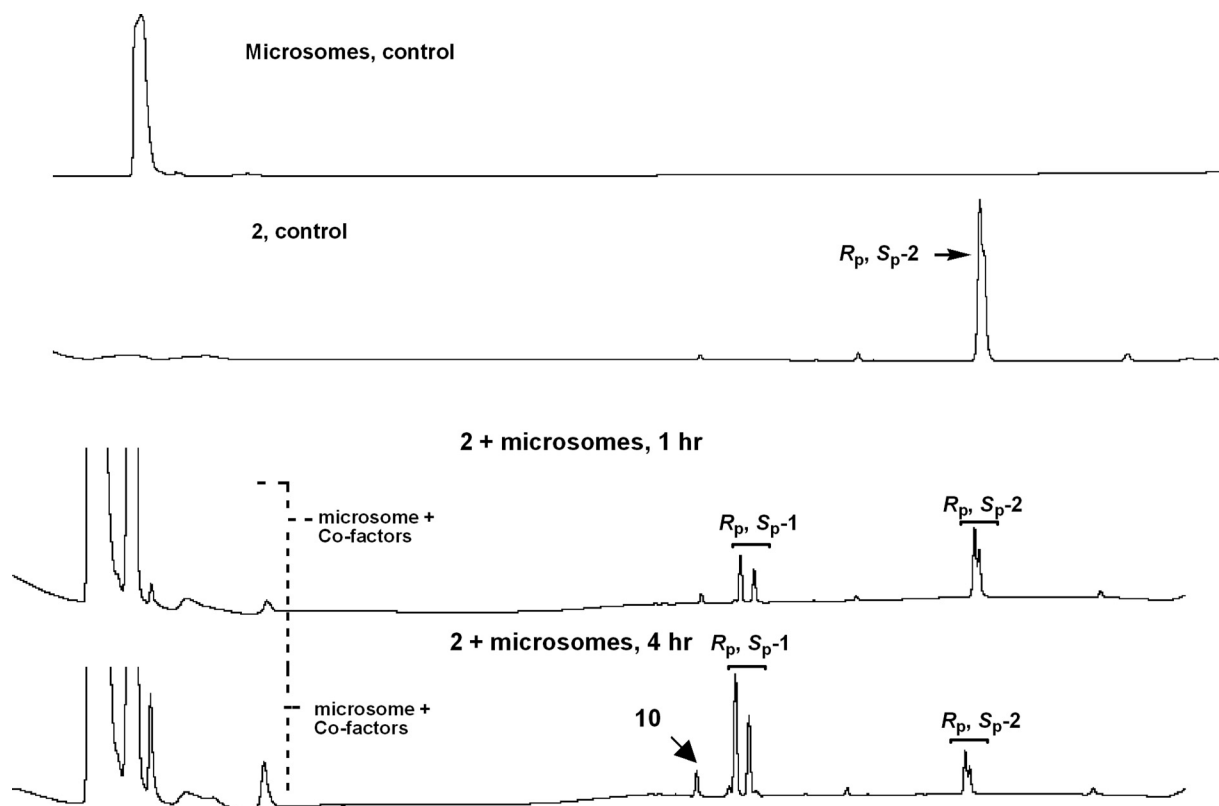
FIG. 2. Representative HPLC profile at different time points of aliquots from the incubation of R_p, S_p-**2** with liver microsomes.

concentration and specific activity. [^{35}S]**2** was added to the unlabeled drug formulation (under reduced light conditions) to give the correct final drug and radioactivity concentration. Dose formulations were prepared fresh at room temperature on the day of administration and were used within 2 h.

Experimental Procedures (In-Life Evaluations). Mortality/morbidity evaluations were performed at least once daily, and animals were examined for clinical signs related to the pharmacology and toxicology of the test article, gross motor and behavioral activity, and observable changes in appearance. Urine and feces were collected ~1, 4, and 24 h postdose. Blood (~200–300 μl) was collected from the retro-orbital sinus under 60% CO_2/40% O_2 anesthesia, just before necropsy, into tubes containing EDTA in wet ice. To generate plasma, samples were centrifuged within 15 min of collection at 1750g for 6 to 8 min. Plasma and whole blood were transferred to cryovials and stored at −20°C for storage until analysis for radioactivity.

All animals were euthanized at their scheduled sacrifice with an overdose of sodium pentobarbital administered intraperitoneally at 1, 4, or 24 h. Liver, lung, kidney, heart, brain, spleen, and tail were collected and stored frozen at

approximately −20°C. The tissues were analyzed for radioactivity by liquid scintillation counting after homogenization and treatment with a tissue solubilizer. Total radioactivity (disintegrations per minute) was determined and calculated as a concentration (microgram-equivalent per milliliter or gram) and as a percentage of the administered dose.

The total radioactivity in plasma, presented as microgram-equivalent per milliliter, was also evaluated using WinNonlin Professional (version 5.2; Pharsight, Mountain View, CA), noncompartmental approaches with sparse sampling feature to determine the elimination $t_{1/2}$, time to maximal plasma concentration, observed maximal plasma concentration (C_{max}), and area under the plasma concentration-time profile (AUC). C_{max} and AUC were presented as the mean ± S.E. of the data.

Results

Synthesis of Compounds. The prodrug **2** was prepared by chemoselective *S*-alkylation of the dinucleotide **1** (Fig. 1). For our studies,
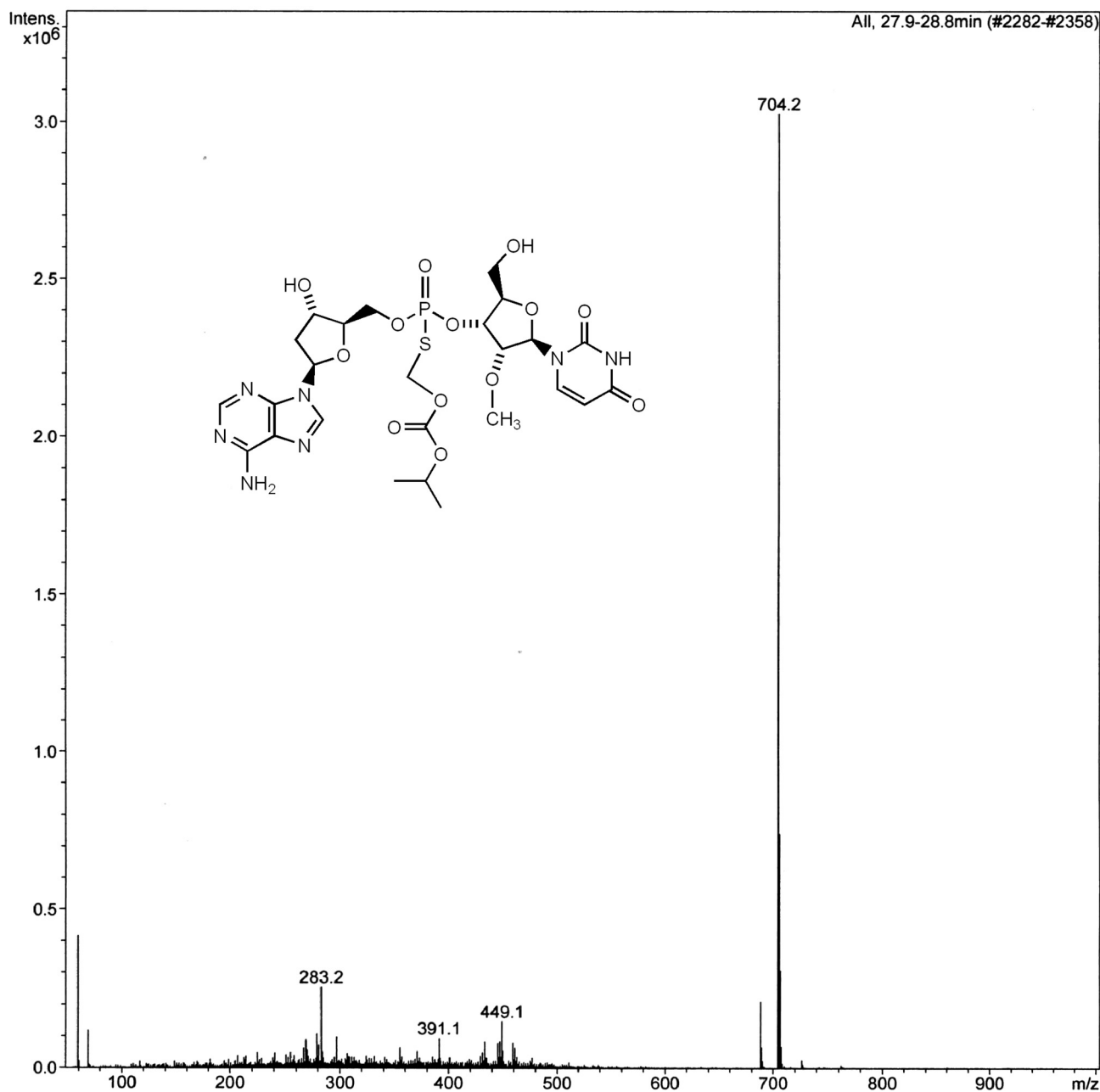

FIG. 3. Mass spectrum of the prodrug **2**. Peak at 704 represents the [M + H] ion.

we used the ~55:45 R_p/S_p mixture of **1**, which was synthesized in large scale using nucleoside-loaded CPG support in conjunction with solid-phase phosphoramidite chemistry, using a specially fabricated LOTUS reactor. In brief, the dA-linked CPG support was prepared using our recently developed ultrafast functionalization and loading process for solid supports. Coupling of the 2′-OMe uridine phosphoramidite to the dA-loaded support was achieved using a solution of ETT as a coupling reagent. The sulfurization of the internucleotidic dinucleoside phosphite-coupled product **5** was performed using 3*H*-1,2-benzodithiole-3-one-1,1,-dioxide. After processing, chromatographic purification, and lyophilization, the sodium salt of R_p,S_p-**1** (~60:40 mixture) was obtained, which was characterized by ^{31}P and ^{1}H NMR and was >96% pure.

The chemoselective *S*-alkylation of R_p,S_p-**1** with iodomethyl isopropyl carbonate gave the prodrug R_p,S_p-**2**. In turn, the iodomethyl

carbonate was prepared by halogen exchange reaction with the corresponding chloro-compound as described previously (Padmanabhan et al., 2006). After HPLC purification and lyophilization, **2** was obtained in overall isolated yields of 50 to 52% from **1**. ^{31}P NMR of **2** showed two peaks representing a ~55:45 ratio of the R_p/S_p isomers, and the mass spectrum was consistent with the expected molecular ion of 703 for **2**.

In Vitro Metabolic Studies of 2 Using Liver Microsomes. The metabolism protocols followed were essentially as described previously (Dalvie et al., 2009), with slight modifications. Thus, exposure of the prodrug R_p, S_p-**2** to liver microsomes up to 8 h resulted in its stereospecific conversion to the dinucleotide R_p, S_p-**1** (Fig. 2). Indeed, the LC/MS evaluation of the microsomal incubate revealed that the major product(s) of metabolism was the R_p, S_p-dinucleotide **1** (Figs. 3 and 4). A minor amount of the desulfurized product **10** (<5%) was
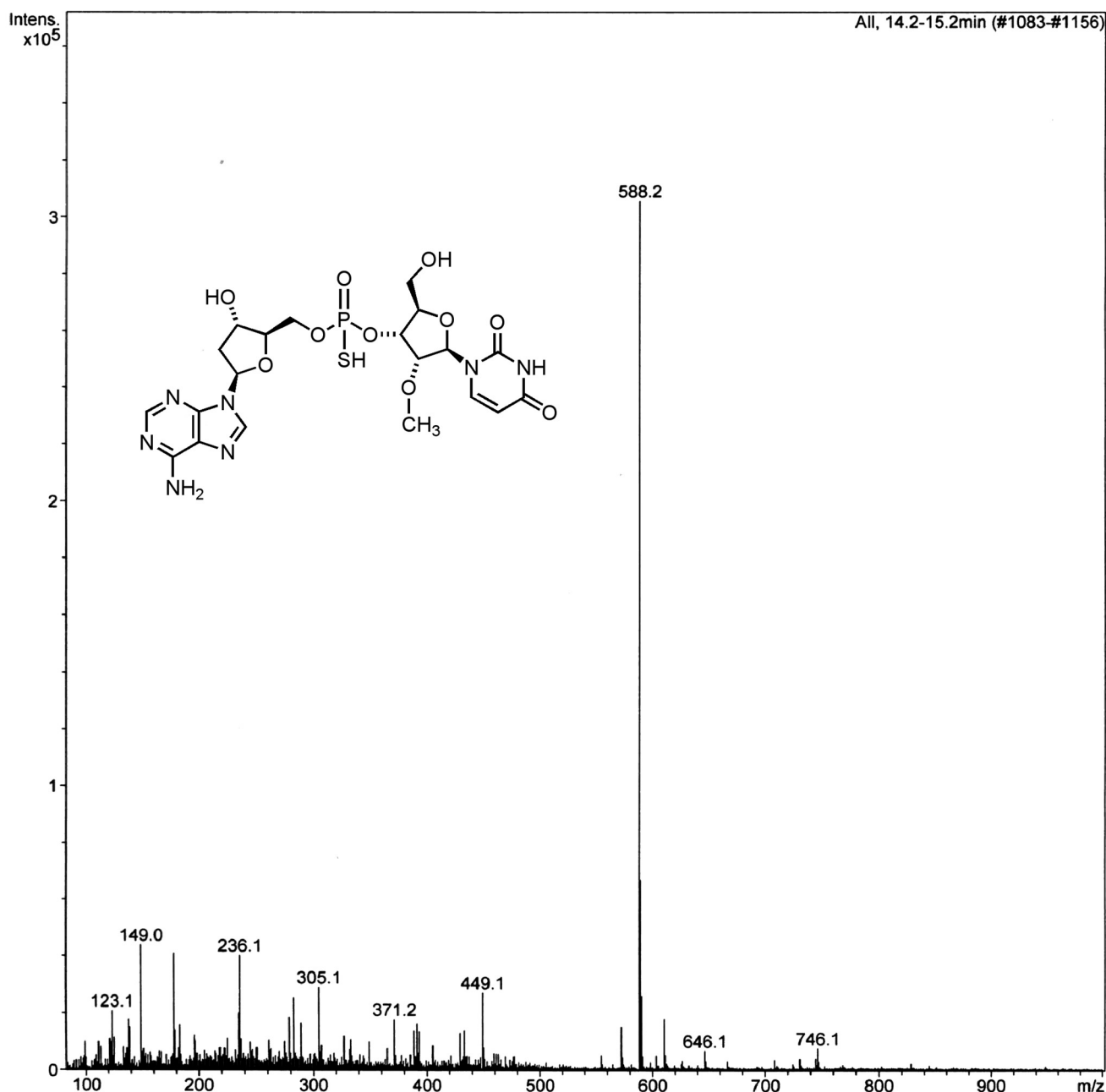

FIG. 4. Mass spectrum of the dinucleoside phosphorothioate **1** resulting from the metabolism of **2** by liver microsomes. The peak at 588 Da represents the [M + H] ion.

also detected as determined by MS analysis (m/e, 571) (Fig. 5). A few minor metabolites (<10%) were also seen (Fig. 2). However, the identity of these metabolites could not be firmly established on the basis of molecular ion. There was no evidence for any quantifiable formation of the deaminated analog **9** (the inosine analog corresponding to **1** that could be formed by the action of *adenosine deaminase*). The absence of **9** was additionally confirmed by independent synthesis and cochromatography along with the metabolite incubate. None of the other predicted metabolites (Fig. 6) such as O-dealkylated ribonucleoside analog of **2** (i.e., **10**) or that of **1** and the 8-oxo-deoxyadenosine analog of **1** (i.e., **11**) and **2** (i.e., **12**) was apparent on the basis of molecular ion analysis in LC/MS. Our curiosity in the formation of **11** and **12** was triggered by the reported susceptibility of position 8 of purine nucleosides to oxidation (Ahmad and Mond, 1985). In addition, there was no apparent formation of 5′-phosphor-

ylated derivatives of **1** or other phase II conjugation products. In all cases, in the microsomal metabolism, both R_p and S_p isomers of prodrug **2** underwent stereospecific conversion to the active **1** with only minor amounts of desulfurized product (**10**) (corresponding to **1**) being observed (Fig. 5). It was also gratifying to find that there appears to be no significant rate differences in the conversion of the individual R_p and S_p isomers of **2** to R_p and S_p isomers of **1**, respectively. These results are consistent with serum-mediated bioreversibility studies previously reported by us (Coughlin et al., 2010).

Similar to the serum-mediated conversion of **2** to **1** in the case of microsomes, liver esterases appear to be the major metabolizing enzymes involved in the hydrolytic conversion of **2** to **1**. Mechanistically, it appears that the formation of **1** from **2** occurs by nucleophilic attack of the serine hydroxyl group of the esterase on the carbonyl carbon of **2** to give **11**, followed by the intramolecular attack of the
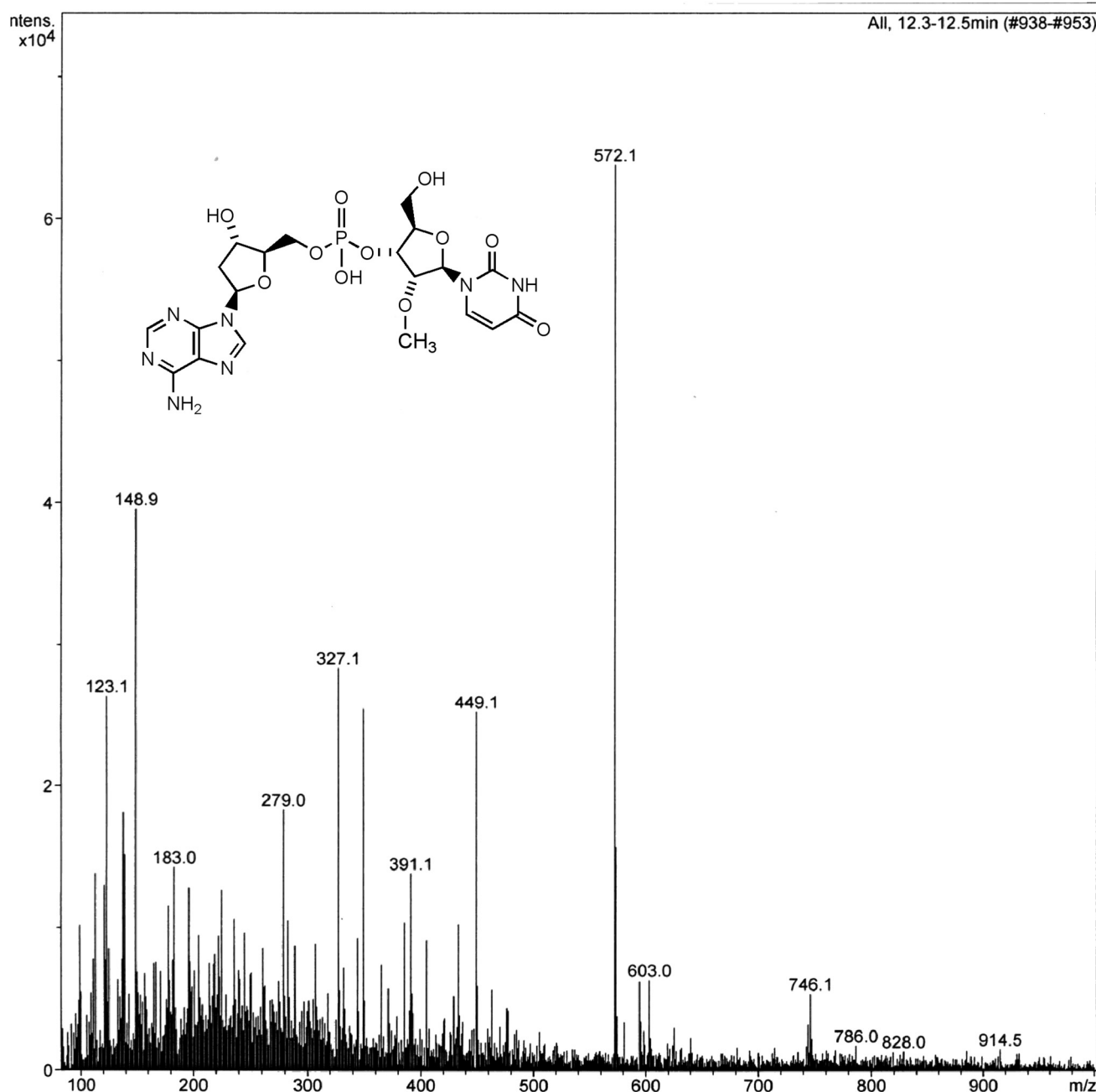

FIG. 5. Mass spectrum of the desulfurized product 10 resulting from the metabolism of 2 by liver microsomes. The peak at 572.1 Da represents the [M + H] ion.
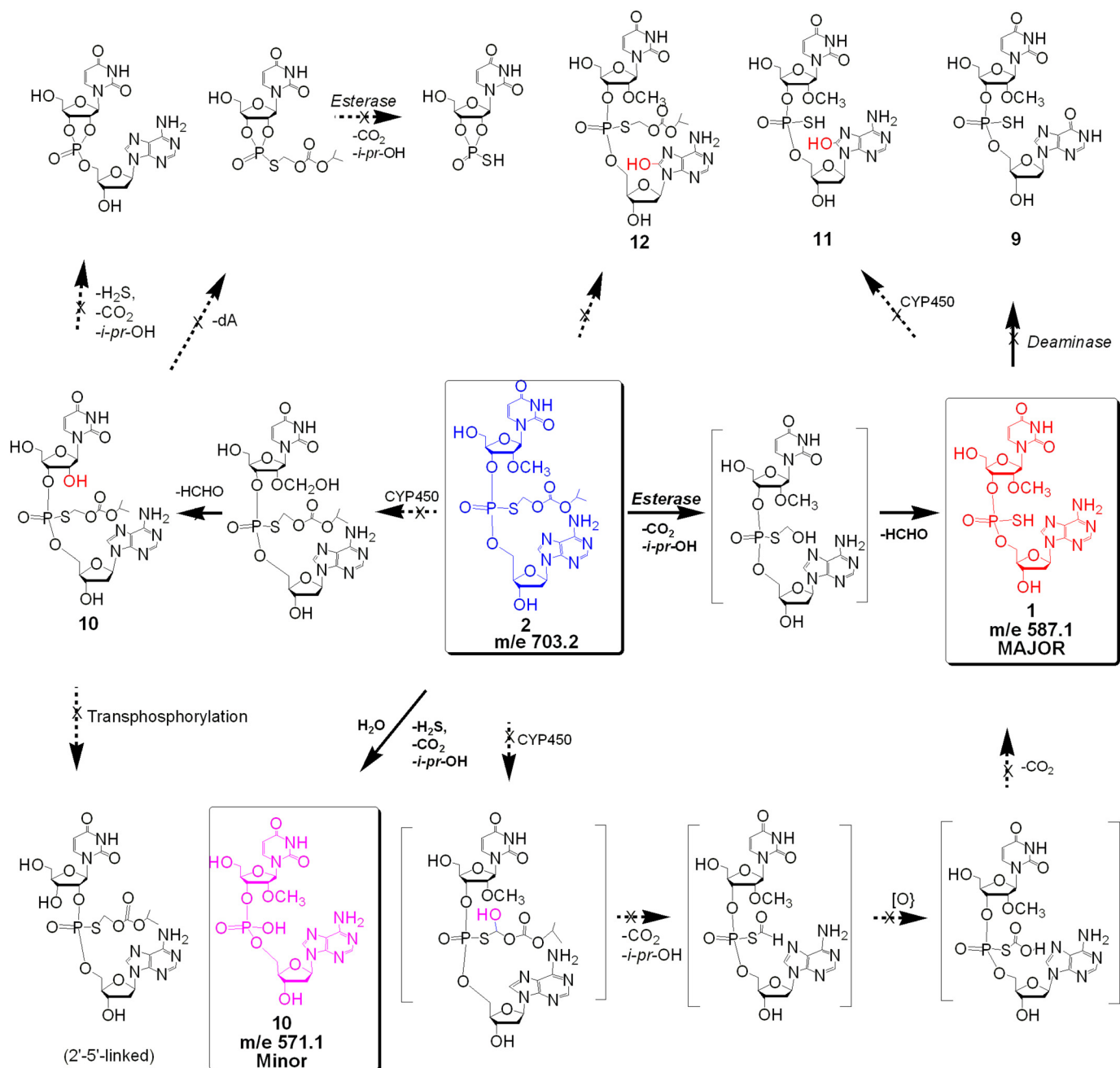
FIG. 6. Predicted pathways for phase I biotransformation of R_p-,S_p-2 by liver microsomes.

incipient oxyanion on the phosphoryl group to give the cyclic intermediate 12 (Fig. 7). The transient species 12 could reorganize to give the trigonal bipyramidal intermediates 13 and 14 that could interconvert by pseudorotation (Westheimer, 1968). Although in the intermediate 14, the S-acyloxyalkyl group is favorably poised to depart from an apical direction (that could cause the formation of desulfurized product 10), its formation is presumably disallowed because of the energetics involved in the reorganization of the initially formed enzyme-substrate complex 12. Consequently, the hydrolytic pathway is directed to occur via 13 to yield the desired 1 with minimal formation of 10. It appears that the 2'-OMe substituent in the dinucleotide structure facilitates hydrolysis of the ester group in each of the isomers with almost equal ease. We hypothesize that the 2'-OMe substitution in the furanose ring of R_p-, S_p-2 favors a $C_{3'}$-endo versus a $C_{2'}$-endo conformation that might optimally orient the ester group in both isomers for enzyme-mediated nucleophilic attack with

equal ease. In our earlier bioreversibility studies of R_p-, S_p-2 using serum, we have found that the individual isomers are stereospecifically converted to R_p-, S_p-1 at almost equal rates (Coughlin et al., 2010). However, the bioreversion of the corresponding S-alkyl derivatives of the dinucleotides 3',5'-linked thymidine-thymidine phosphorothioate and 3',5'-linked deoxyadenosine-thymidine phosphorothioate-5' (both of which lack the 2'-OMe substituent) occurs with significant rate differences between R_p and S_p isomers (Padmanabhan et al., 2006; Coughlin et al., 2010). These results suggest that subtle conformational effects are in play in the enzyme-mediated hydrolysis of 2. The facile bioconversion of 2 to 1 in liver and plasma is also consistent with broad substrate specificity of the ubiquitous esterase enzymes.

In Vitro Metabolism of 2 by S9 Fractions. Similar to liver microsomal studies, exposure of the prodrug 2 to S9 fractions also resulted in stereospecific conversion of 2 to the dinucleotide 1 (Supplemental Fig. 2).

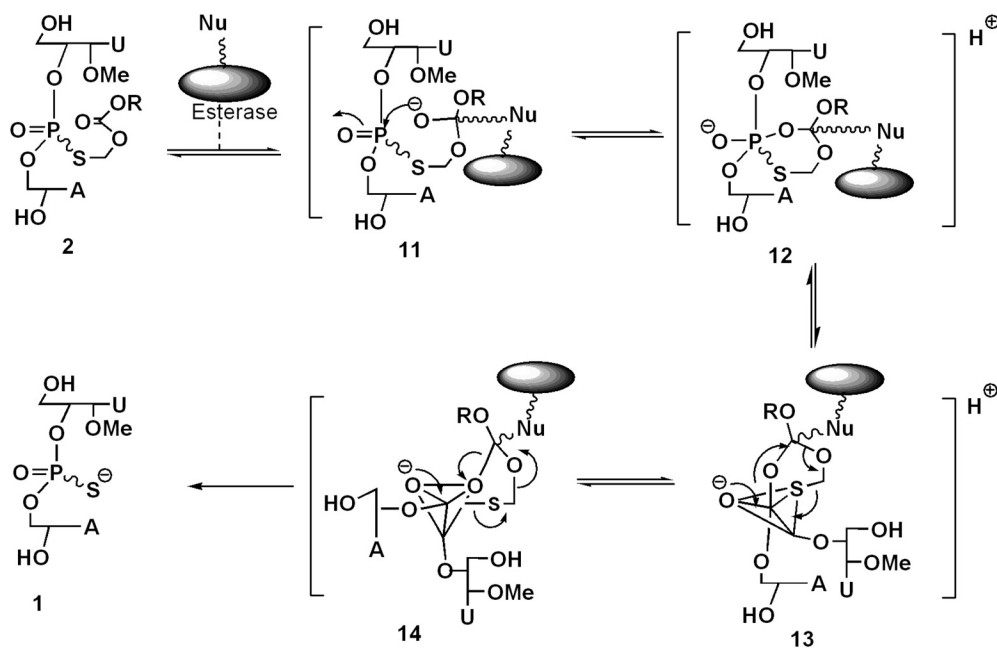FIG. 7. Proposed mechanism of bioconversion of R_p-, S_p-**2** to Rp-, Sp-**1** by liver esterases. The proposed mechanism is based on an earlier publication (Coughlin et al., 2010) and references cited therein.

Evaluation of the incubate by LC/MS revealed that besides the major product **1**, minor amounts of the desulfurized product **10** (<5%) were also formed. A few minor metabolites were also observed. The pattern of metabolites was similar to that observed with liver microsomes. There was no apparent evidence of any phase II conjugative reactions of **2** or that of the initially formed active metabolite **1**.

Stability Studies of 2 in SGF and SIF. An important requirement for oral bioavailability of the prodrug **2** is its stability in gastric fluid. Given the known susceptibility of the dinucleotide **1** to acid-catalyzed decomposition, it was not known whether **2** would have adequate stability gastric fluid. Therefore, we evaluated the stability of **2** and the dinucleotide **1** in SGF and SIF by HPLC analysis of aliquots at different time points. Whereas the dinucleotide **1** decomposed rapidly in SGF ($t_{1/2} < 15$ min), we were gratified to find that the prodrug **2** displayed high stability in SGF with $t_{1/2} > 3$ h (Fig. 8). In SIF, **2** was almost completely converted to **1** in ~3 h, whereas **1** was stable in SIF (Supplemental Fig. 3). Our stability data on prodrug **2** is consistent with that reported for S-acyl-2-thioethyl pronucleotides (Shafiee et al., 2001). However, the mechanistic rationale for the greater stability of **2** in SGF compared with **1** is not established as yet.

Tissue Distribution and Excretion of [³⁵S]2. Each rat was administered [³⁵S]**2**, 10 mg/kg, by either the intravenous or the oral route. The intravenous dose of radioactivity was 15.5 ± 0.64 (males) and 14.2 ± 0.15 μCi (females). The oral dose of radioactivity was 50.1 ± 0.91 (males) and 48.0 ± 2.02 μCi (females). The total recovery of radioactivity determined at 24 h after intravenous administration of [³⁵S]**2** was 83.7 ± 0.32 and $84.9 \pm 0.36\%$ for male and female rats and after oral administration was 83.0 ± 3.59 and $80.4 \pm 6.79\%$ for male and female rats, respectively.

Table 1 summarizes the excretion of radioactivity after intravenous and oral dosing of [³⁵S]**2**. After intravenous administration of [³⁵S]**2**, approximately 20% of the dose was excreted in the urine in the first hour. In both males and females, the major route of excretion after intravenous dosing was in the urine (55–60% of the radioactive dose), whereas approximately 10 to 20% of the dose was excreted in the feces in 24 h. Oral administration of [³⁵S]**2** resulted in 35 to 40% of the dose eliminated in the urine in 24 h. In male rats, a similar fraction of the dose was excreted in the feces, whereas female rats excreted a much smaller fraction in the feces, ~3% in 24 h.

A larger fraction of the total dose of radioactivity was found in the carcass of females in the oral group (and the intestines were observed to contain more fecal material), suggesting that excretion by this route is probably similar in male and female rats, but that females had not yet eliminated feces during the study period. Comparing the same time points, the highest fraction of the dose was present in liver > blood $\approx$ plasma > kidney > lung, after both intravenous and oral administration. Brain, spleen, and heart had 0.5% or less of the dose at all time points and for both intravenous and oral routes of administration. Supplemental Figs. 4 and 5 are graphical representations of the time course of the presence of radioactivity in the principal tissues in male and female rats, respectively. After intravenous administration, the concentration of radioactivity in liver and kidney was higher than that of the plasma levels at the three time points 1, 4, and 24 h, whereas lung had a similar concentration of radioactivity compared with that of plasma. After oral administration of [³⁵S]**2**, the highest concentration of radioactivity was observed at 4 h postdose. On the basis of the concentration ratios of tissue/plasma, radioactivity from [³⁵S]**2** tended to concentrate in the liver and kidney after both intravenous or oral administration (Fig. 9). The time of peak concentration after an oral dose was 4 h for plasma, blood, and tissues. Tissue distribution evaluation demonstrated that the radioactivity concentrates in the liver, with the highest liver/plasma ratio in the intravenous group at 1 h, 3.89 (females), and in the oral group at 1 h, 2.86 (males).

Table 2 summarizes the pharmacokinetic parameters for total radioactivity in plasma, calculated as microgram-equivalent per milliliter. The elimination $t_{1/2}$ for radioactivity after an intravenous dose was 8 to 9 h. The observed C_{max} of radioactivity was approximately 2.5 μg-Eq/ml in the oral dose group at 4 h and approximately twice that in the intravenous group at 0.25 h. The ratio of the AUC in the oral dose group to AUC in the intravenous dose group was 0.50 and 0.78 for males and females, respectively.

Although individual fractions from tissues and plasma at different time points were not analyzed by radio-HPLC, on the basis of the metabolism and stability studies of **1** and **2**, it is reasonable to assume that the radioactivity in tissues and plasma corresponds mostly to that of [³⁵S]**1** or [³⁵S]**2** and minimally to ³⁵S-containing metabolites or elemental ³⁵S.
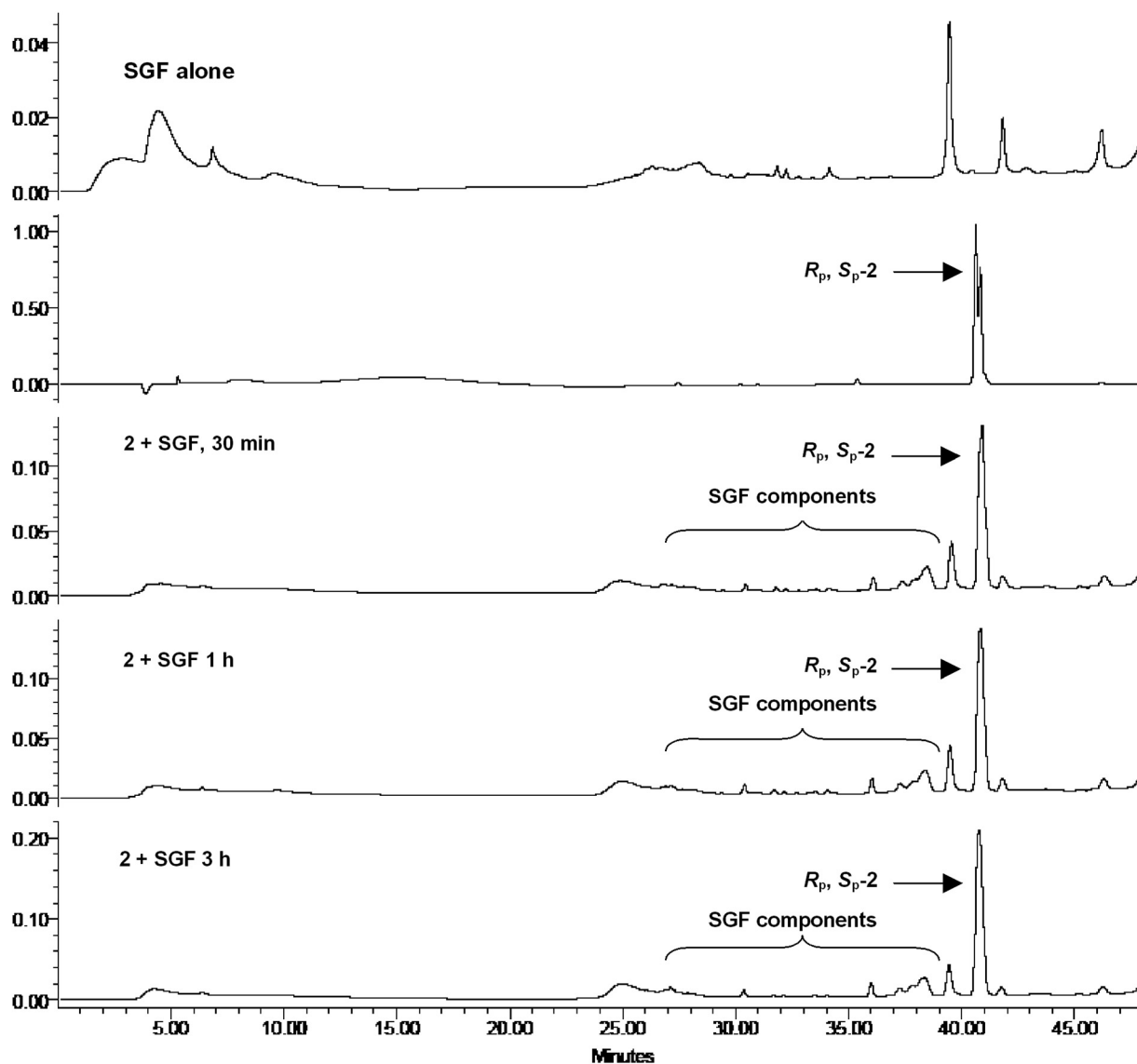
Fig. 8. Representative time course HPLC profiles of incubates of R_p-, S_p-2 in SGF that demonstrates the stability of 2 in the acidic environment of stomach.

Discussion

The studies described in this article were undertaken as part of the preclinical development of a prodrug 2 of the dinucleoside phosphorothioate 1, a representative SMNH compound, having anti-HBV activity. Metabolic studies of R_p-, S_p-2 using liver microsomes and S9 fractions show that it is stereospecifically converted to R_p-,S_p-1 via hydrolysis mediated by esterases. Neither 2 nor 1 was susceptible to oxidative metabolism by P450- or exo- and endo-nuclease-mediated fragmentation. Furthermore, there was no evidence of phase II conjugation reactions. The prodrug 2 was quite stable in SGF compared with the dinucleotide 1.

Tissue distribution studies of orally and intravenously administered [^{35}S]2 demonstrated that the radioactivity concentrates in the liver. According to the metabolic studies, it is likely that most of the radioactivity in the liver is associated with either [^{35}S]2 or [^{35}S]1. The preferential distribution of the dinucleotide 1 and its prodrug 2 into liver may be attributed to the presence of nucleoside phosphorothioate backbone because PS-ODN also reveal similar tissue distribution profile upon intravenous administration (Geary, 2009).

The dinucleoside phosphorothioate prodrug 2 is quite stable in SGF and appears to be less stable in SIF where it is converted to the active

1. In acidic pH, 2 is likely to be protonated in the ring nitrogen of adenine, and consequently 2 may not be absorbed from stomach by passive diffusion. It is hence likely that oral absorption of the prodrug 2 occurs predominantly in the upper duodenal region where a significant portion of the molecule may be in the un-ionized form. It is not known whether nucleotide transporters in the gastrointestinal tract have any role in the active transport-mediated absorption of 2 and 1 (Ritzel et al., 2001; Zheng et al., 2004).

These observations further support the hypothesis that the observed anti-HBV activity of 1 and 2 (Iyer et al., 2004a,b; Coughlin et al., 2010) is associated with the intact dinucleotide structure. The tissue distribution studies show that after the oral administration of 2 in rats, the compound is rapidly absorbed and is readily distributed significantly to the liver, the target organ for HBV. The compound is converted rapidly to the active 1 via plasma and/or liver esterases and is concentrated in the liver. Once inside the cell, it is possible that the negatively charged 1 remains trapped in the intracellular compartment and is made available for sustained antiviral effect.

The metabolism and tissue distribution studies of the prodrug 2 have revealed a number of interesting findings that may have impli-

TABLE 1

Excretion data after oral and intravenous administration of [³⁵S]2

Data are presented as mean and S.D. values derived at each time point from nine male and nine female rats.

Route	Sex	Time	Urine		Feces	
		h	% of dose mean	S.D.	% of dose mean	S.D.
Intravenous	M	0–1	22.83	NC	NS	NC
		1–4	11.33	6.72	0.01	NC
		4–24	29.60	11.46	16.90	4.57
		0–24	56.15	5.13	16.90	4.57
Intravenous	F	0–1	15.81	5.16	NS	NC
		1–4	6.34	2.86	NS	NC
		4–24	36.79	1.11	9.44	0.18
		0–24	58.94	1.87	9.44	0.18
	M	0–1	NS	NC	0.01	NC
Oral		1–4	0.86	0.33	0.01	NC
		4–24	33.73	5.20	35.71	7.40
		0–24	34.59	5.14	35.71	7.40
Oral	F	0–1	0.16	NC	0.02	NC
		1–4	2.04	1.20	0.08	NC
		4–24	34.78	5.31	2.68	2.31
		0–24	36.88	6.26	2.72	2.34

M, male; F, female; NC, not calculated; NS, not significant.

cations in the ADME of the longer chain PS-ODN counterparts. As mentioned before, ADME studies of PS-ODN and oligos with different chemical modifications reveal a "class pattern" in which after intravenous administration, they are rapidly cleared from plasma after absorption and are preferentially distributed to liver, kidney, spleen, and bone marrow. In contrast, our evaluation of ADME properties of SMNH compounds reveals that they are preferentially distributed in liver and kidney with less distribution to other tissues. Our studies suggest that distribution to tissue compartments other than liver and kidney may depend on the length and charge of the PS-ODN.

In toxicology studies, intravenous administration of PS-ODN shows a number of dose-dependent effects such as complement activation, splenomegaly, elevation of liver transaminases, lymphoid hyperplasia, immune stimulation manifested as multiorgan mixed mononuclear cell infiltrate with fibroblast proliferation, increased IgM, cytokine production, etc. that are charge- and sequence-dependent as well as species-dependent (Henry et al., 1997, 1999). siRNA is also known to induce immune-stimulatory effects via activation of Toll-like receptors 7 and 8 (Marques and Williams, 2005) that constitute one of their important off-target effects. On the other hand, 7- and 14-day dose-ranging toxicology and toxicokinetic studies of **2** do not show these toxicological characteristics (C. E. Green, K. G. O'Loughlin, J. Marquis, R. P. Iyer, and J. C. Mirsalis, unpublished results) that are hallmarks of PS-ODN and siRNA.

PS-ODN and siRNA are primarily metabolized by *exo-* and *endo*nucleases into shorter ODN fragments and are excreted primarily through kidneys. It is possible that most of the ODNs are metabolized eventually into much shorter fragments including dinucleotides, which are then eliminated. In this context, it is pertinent to mention that PS-ODNs, including those that carry additional sugar modifications, appear to be retained in the tissues over extended periods and slowly metabolized predominantly in liver and kidney over time. Although several reports of metabolic studies of ODN with different sequences and chemical modifications have been reported (Geary, 2009), the biological effects and fate of the shorter fragments that result from metabolism of the parent ODN remain largely unknown. Our studies show that SMNH compounds, particularly dinucleotides, may represent the terminal fragments of nuclease-mediated metabolism of longer chain ODNs.

Furthermore, as described before, SMNH analogs have a variety of biological activities. We have found (Iyer et al., 2010) that certain SMNH analogs can activate cellular cytosolic pathogen recognition receptors such as retinoic acid-inducible gene (RIG-I) (Katze et al., 2002; Akira et al., 2006; Saito et al., 2007; Myong et al., 2009) and nucleotide oligomerization domain protein 2 (Sabbah et al., 2009; Ting et al., 2010) that cause stimulation of innate immune pathways, interferon production and induction of antiviral state (Saito et al., 2007).

In conclusion, ADME studies of SMNH compounds suggest that they 1) are not subject to P450 metabolism and 2) can be delivered orally via a prodrug strategy. In addition, the prodrug derivatization facilitates distribution into the liver, the target organ for hepatitis viruses. A greater understanding of biological activities of SMNH analogs may help to design ODNs with minimal off-target effects for application as antisense, RNA interference, aptamers, and immunomodulatory compounds. Fur-
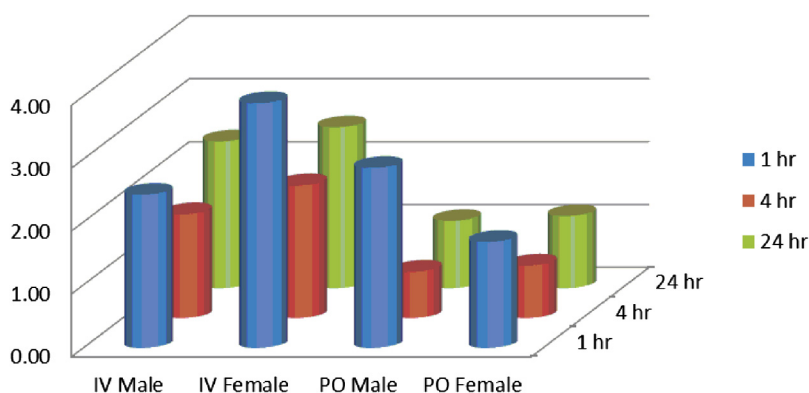
FIG. 9. Ratio of liver to plasma radioactivity concentration after intravenous and oral administration of [³⁵S]**2** in male and female rats. Data is presented as mean values derived at each time point from nine male and nine female rats.

TABLE 2

Pharmacokinetic parameters for total radioactivity in plasma after oral and intravenous administration of [^{35}S]2

Data are presented as mean ± S.D. values derived at each time point from nine male and nine female rats.

Parameter	Intravenous Dose		Oral Dose	
	Male	Female	Male	Female
$t_{1/2}$, h	7.8	9.0	NC	NC
T_{max}, h	NA	NA	4	4
C_{max}, μg-Eq/ml	6.51 ± 0.60	4.49 ± 0.16	2.53 ± 0.30	2.50 ± 0.22
$C_{max p.o.}/C_{max i.v.}$	NA	NA	0.39	0.56
AUC, h-μg-Eq/ml	53.58 ± 1.37	35.21 ± 3.23	26.86 ± 3.52	27.37 ± 2.52
$AUC_{p.o.}/AUC_{i.v.}$	NA	NA	0.50	0.78

NC, not calculated; NA, not applicable; $AUC_{p.o.}$, area under the plasma concentration-time profile with oral dose administration; $AUC_{i.v.}$, area under the plasma concentration-time profile with intravenous dose administration.

ther studies on the preclinical development of SMNH compounds are planned and results will be reported in due course.

Authorship Contributions

Participated in research design: Pandey, Padmanabhan, Marquis, Green, Mirsalis, and Iyer.

Conducted experiments: Coughlin, Pandey, Padmanabhan, O'Loughlin, and Iyer.

Contributed new reagents or analytic tools: Coughlin and Pandey.

Performed data analysis: Coughlin, Pandey, Padmanabhan, Green, and Iyer.

Wrote or contributed to the writing of the manuscript: Iyer, Pandey, Padmanabhan, Marquis, and Mirsalis.

References

Agrawal S, Zhang X, Lu Z, Zhao H, Tamburin JM, Yan J, Cai H, Diasio RB, Habus I, and Jiang Z (1995) Absorption, tissue distribution and in vivo stability in rats of a hybrid antisense oligonucleotide following oral administration. *Biochem Pharmacol* **50:**571–576.

Ahmad A and Mond JJ (1985) 8-Hydroxyguanosine and 8-methoxyguanosine possess immunostimulating activity for B lymphocytes. *Cell Immunol* **94:**276–280.

Akira S, Uematsu S, and Takeuchi O (2006) Pathogen recognition and innate immunity. *Cell* **124:**783–801.

Beaucage SL and Iyer RP (1992) Advances in the synthesis of oligonucleotides by the phosphoramidite approach. *Tetrahedron* **48:**2223–2311.

Coughlin JE, Padmanabhan S, Zhang G, Kirk CJ, Govardhan CP, Korba BE, O'Loughlin K, Green CE, Mirsalis J, Morrey JD, et al. (2010) Orally bioavailable anti-HBV dinucleoside acyloxyalkyl prodrugs. *Bioorg Med Chem Lett* **20:**1783–1786.

Crooke RM, Graham MJ, Martin MJ, Lemonidis KM, Wyrzykiewicz T, and Cummins LL (2000) Metabolism of antisense oligonucleotides in rat liver homogenates. *J Pharmacol Exp Ther* **292:**140–149.

Dalvie D, Obach RS, Kang P, Prakash C, Loi CM, Hurst S, Nedderman A, Goulet L, Smith E, Bu HZ, et al. (2009) Assessment of three human in vitro systems in the generation of major human excretory and circulating metabolites. *Chem Res Toxicol* **22:**357–368.

Dias N and Stein CA (2002) Antisense oligonucleotides: basic concepts and mechanisms. *Mol Cancer Ther* **1:**347–355.

Ellington AD and Conrad R (1995) Aptamers as potential nucleic acid pharmaceuticals. *Biotechnol Annu Rev* **1:**185–214.

Geary RS (2009) Antisense oligonucleotide pharmacokinetics and metabolism. *Expert Opin Drug Metab Toxicol* **5:**381–391.

Gibaldi M, Boyes RN, and Feldman S (1971) Influence of first-pass effect on availability of drugs on oral administration. *J Pharm Sci* **60:**1338–1340.

Hannon GJ (2002) RNA interference. *Nature* **418:**244–251.

Hannoush RN, Min KL, and Damha MJ (2004) Diversity-oriented solid-phase synthesis and biological evaluation of oligonucleotide hairpins as HIV-1 RT RNase H inhibitors. *Nucleic Acids Res* **32:**6164–6175.

Henry SP, Monteith D, and Levin AA (1997) Antisense oligonucleotide inhibitors for the treatment of cancer: 2. Toxicological properties of phosphorothioate oligodeoxynucleotides. *Anticancer Drug Des* **12:**395–408.

Henry SP, Templin MV, Gillett N, Rojko J, and Levin AA (1999) Correlation of toxicity and pharmacokinetic properties of a phosphorothioate oligonucleotide designed to inhibit ICAM-1. *Toxicol Pathol* **27:**95–100.

Institute of Laboratory Animal Resources (1996) *Guide for the Care and Use of Laboratory Animals* 7th ed. Institute of Laboratory Animal Resources, Commission on Life Sciences, National Research Council, Washington DC.

Iyer RP, Regan JB, Egan W, and Beaucage SL (1990a) 3H-1,2-benzodithiol-3-one 1, 1-dioxide as an improved sulfurizing reagent in the solid-phase synthesis of oligodeoxyribonucleoside phosphoramidites. *J Am Chem Soc* **112:**1253–1254.

Iyer RP, Phillips LR, Egan W, Regan JB, and Beaucage SL (1990b) The automated synthesis of sulfur-containing oligodeoxyribonucleotides using 3H-1,2-benzodithiol-3-one-1, 1-dioxide as a sulfur-transfer reagent. *J Org Chem* **55:**4693–4699.

Iyer RP, Tan W, Yu D, and Agrawal S (1994) Synthesis of [^{35}S]-3H-1, 2-benzodithiol-3-one-1,1-dioxide: application in the preparation of site-specifically ^{35}S-labeled oligonucleotides. *Tetrahedron Lett* **35:**9521–9524.

Iyer RP, Jin Y, Roland A, Morrey JD, Mounir S, and Korba B (2004a) Phosphorothioate di- and trinucleotides as a novel class of anti-hepatitis B virus agents. *Antimicrob Agents Chemother* **48:**2199–2205.

Iyer RP, Roland A, Jin Y, Mounir S, Korba B, Julander JG, and Morrey JD (2004b) Anti-hepatitis B virus activity of ORI-9020, a novel phosphorothioate dinucleotide, in a transgenic mouse model. *Antimicrob Agents Chemother* **48:**2318–2320.

Iyer RP, Coughlin JE, and Padmanabhan S (2005a) Rapid functionalization and loading of solid supports. *Org Prep Proc Int* **37:**205–212.

Iyer RP, Padmanabhan S, Zhang G, Morrey JD, and Korba BE (2005b) Nucleotide analogs as novel anti-hepatitis B virus agents. *Curr Opin Pharmacol* **5:**520–528.

Iyer RP, Coughlin J, and Padmanabhan S (2006) Metabolism and pharmacokinetic studies of SB 9000–a novel anti-HBV agent. *Abstracts of the 19th International Conference on Antiviral Research*; 2006 Apr 29–May 3; Palm Springs, CA. International Society for Antiviral Research, Washington, DC.

Iyer RP, Coughlin, JE, Padmanabhan S, Korba, BE, and Myong S (2010) Activation of retinoic acid inducible gene (RIG-I) by nucleotide analogs–a potential novel mechanism for antiviral discovery. *Abstracts of the 23rd International Conference on Antiviral Research*; 2010 Apr 25–27; San Francisco, CA. International Society for Antiviral Research, Washington, DC.

Katze MG, He Y, and Gale M Jr (2002) Viruses and interferon: a fight for supremacy. *Nat Rev Immunol* **2:**675–687.

Li J and Liang Z (2010) The consideration of synthetic short interfering RNA for therapeutic use. *Basic Clin Pharmacol Toxicol* **106:**22–29.

Marques JT and Williams BR (2005) Activation of the mammalian immune system by siRNAs. *Nat Biotechnol* **23:**1399–1405.

Myong S, Cui S, Cornish PV, Kirchhofer A, Gack MU, Jung JU, Hopfner KP, and Ha T (2009) Cytosolic viral sensor RIG-I is a 5′-triphosphate-dependent translocase on double-stranded RNA. *Science* **323:**1070–1074.

Ollis DL and White SW (1987) Structural basis of protein-nucleic acid interactions. *Chem Rev* **87:**981–995.

Padmanabhan S, Coughlin JE, Zhang G, Kirk CJ, and Iyer RP (2006) Anti-HBV nucleotide prodrug analogs: synthesis, bioreversibility, and cytotoxicity studies. *Bioorg Med Chem Lett* **16:**1491–1494.

Padmanabhan S, Coughlin JE, and Iyer RP (2005) Microwave-assisted functionalization of solid supports. Application in the rapid loading of nucleosides on controlled-pore-glass (CPG). *Tetrahedron Lett* **46:**343–347.

Peng B, Andrews J, Nestorov I, Brennan B, Nicklin P, and Rowland M (2001) Tissue distribution and physiologically based pharmacokinetics of antisense phosphorothioate oligonucleotides ISIS 1082 in rat. *Antisense Nucleic Acid drug Dev* **11:**15–27.

Perrillo RP (2004) Overview of treatment of hepatitis B: key approaches and clinical challenges. *Semin Liver Dis* 24 (**Suppl 1**):23–29.

Ritzel MW, Ng AM, Yao SY, Graham K, Loewen SK, Smith KM, Ritzel RG, Mowles DA, Carpenter P, Chen XZ, et al. (2001) Molecular identification and characterization of novel human and mouse concentrative Na+-nucleoside cotransporter proteins (hCNT3 and mCNT3) broadly selective for purine and pyrimidine nucleosides (system cib). *J Biol Chem* **276:**2914–2927.

Sabbah A, Chang TH, Harnack R, Frohlich V, Tominaga K, Dube PH, Xiang Y, and Bose S (2009) Activation of innate immune antiviral responses by Nod2. *Nat Immunol* **10:**1073–1080.

Saito M, Go M, and Shirai T (2006) An empirical approach for detecting nucleotide-binding sites on proteins. *Protein Eng Des Sel* **19:**67–75.

Saito T, Hirai R, Loo YM, Owen D, Johnson CL, Sinha SC, Akira S, Fujita T, and Gale M Jr (2007) Regulation of innate antiviral defenses through a shared repressor domain in RIG-I and LGP2. *Proc Natl Acad Sci USA* **104:**582–587.

Sanger W (1983) *Principles of Nucleic Acid Structure*, Springer-Verlag, New York.

Shafiee M, Deferme S, Villard AL, Egron D, Gosselin G, Imbach JL, Lioux T, Pompon A, Varray S, Aubertin AM, et al. (2001) New bis(SATE) prodrug of AZT 5′-monophosphate: in vitro anti-HIV activity, stability, and potential oral absorption. *J Pharm Sci* **90:**448–463.

Szymkowski DE (1996) Developing antisense oligonucleotides from the laboratory to clinical trials. *Drug Disc Today* **1:**415–428.

Tillman LG, Geary RS, and Hardee GE (2008) Oral delivery of antisense oligonucleotides in man. *J Pharm Sci* **97:**225–236.

Ting JP, Duncan JA, and Lei Y (2010) How the noninflammasome NLRs function in the innate immune system. *Science* **327:**286–290.

Tuschl T (2001) RNA interference and small interfering RNAs. *Chembiochem* **2:**239–245.

The United States Pharmacopeia (1993). The National Formulary 18, 23rd ed, pp 1788–1789, United States Pharmacopeial Convention, Inc., Rockville. United States Pharmacopeia, Washington, DC.

van de Water FM, Boerman OC, Wouterse AC, Peters JG, Russel FG, and Masereeuw R (2006) Intravenously administered short interfering RNA accumulates in the kidney and selectively suppresses gene function in renal proximal tubules. *Drug Metab Dispos* **34:**1393–1397.

Wagner RW, Matteucci MD, Grant D, Huang T, and Froehler BC (1996) Potent and selective inhibition of gene expression by an antisense heptanucleotide. *Nat Biotechnol* **14:**840–844.

Westheimer FH (1968) Pseudo-rotation in the hydrolysis of phosphate esters. *Acc Chem Res* **1:**70–78.

Zheng CJ, Sun LZ, Han LY, Ji ZL, Chen X, and Chen YZ (2004) Drug ADME-associated protein database as a resource for facilitating pharmacogenomics research. *Drug Dev Res* **62:**134–142.

Address correspondence to: Radhakrishnan P. Iyer, Spring Bank Pharmaceuticals, Inc., S-7, 113 Cedar St., Milford, MA 01757. E-mail: kiyer@springbankpharm.com